Supporting Information

Transition Metal Complex Dyes Sensitized 3D Iodoplumbates: Syntheses, Structures and Photoelectric Properties

Cheng-Yang Yue,[a,b,c] Hai-Xiao Sun,[a] Dong-Yang Li,[a] Lu Gao, Na Lin, Xin-Ming Wang, Ying-Xue Jin, Yu-Han Dong, Zhi-Hong Jing,*[b] Xiao-Wu Lei,*[a,b,c]

[a]Department of Chemistry and Chemical Engineering, Jining University, Qufu, Shandong, 273155, P. R. China

[b]College of Chemistry and Chemical Engineering, Qufu Normal University, Qufu, Shandong, 273165, P. R. China

[c]State Key Laboratory of Structural Chemistry, Fujian Institute of Research on the Structure of Matter, Chinese Academy of Sciences, Fuzhou, Fujian, 350002, P. R. China

*_Corresponding author_: Zhi-Hong Jing, Xiao-Wu Lei

E-mail address: zhhjing@126.com; xwlei_jnu@163.com

Experimental Section.

Materials and Instruments. All reagents and solvents were commercially available and used as received without further purification. Elemental analysis was performed on a PE2400 II elemental analyzer. Powder X-ray diffraction (PXRD) data were measured on a Bruker D8 ADVANCE powder X-ray diffractometer (Cu Kα, λ = 1.5418 Å) in the 2θ range of 5–80º. UV−vis absorption was monitored with a PE Lambda 900 UV/vis spectrophotometer in the wavelength range of 200−800 nm. The thermal behavior (TGA) was studied by a Mettler TGA/SDTA 851 thermal analyzer under a N_2 atmosphere with a heating rate of 10 °C min^{-1}. Elemental analyses and mapping were performed on a JSM-6700F scanning electron microscope (SEM) equipped with an energy dispersive X-ray spectroscope (EDS, Oxford INCA).

Syntheses and Reaction. A mixture of KI (0.5 mmol), $FeSO_4·7H_2O$ (0.5 mmol), PbI_2 (3 mmol), 2,2-bipy (1.5 mmol), hydroiodic acid (47%, 0.5 mL), distilled water (4 mL) and dimethylformamid (3 mL) was sealed in a 15-mL Teflon-lined stainless container, which was heated at 140 °C for 6 days. With cooling rate of 5 °C min^{-1} to room temperature, dark red block-shaped crystals were found in 22% yield based on PbI_2 and subsequently determined as $[Fe(2,2\text{-bipy})_3]_2Pb_8I_{21}$. The crystals were easily collected by hand and washed with distilled water and ethanol. Elem. Anal. Calcd for $C_{60}N_{12}H_{49}Fe_2Pb_8I_{21}$: C, 15.01; H, 1.02; N, 2.98 %; found: C, 13.41; H, 0.92; N, 3.13 %. The isostructural phases of Co, Ni and Mn was also synthesized in the analogous manner to that of Fe phase with $Co(CH_3COO)_2·4H_2O$, $Ni(CH_3COO)_2·4H_2O$ and $Mn(CH_3COO)_2·4H_2O$ instead of $FeSO_4·7H_2O$, respectively. The red and orange crystals of Co, and Ni and Mn phases were obtained in yields of 12%, 15 % and 17% based on PbI_2, respectively. Elem. Anal. Calcd for $C_{60}N_{12}H_{49}Co_2Pb_8I_{21}$: C, 13.57; H, 0.90; N, 3.66; found: C, 13.40; H, 0.92; N, 3.13 %; $C_{60}N_{12}H_{49}Ni_2Pb_8I_{21}$: C, 13.28; H, 0.88; N, 3.47 %; found: C, 13.41; H, 0.92; N, 3.13 %; $C_{60}N_{12}H_{49}Mn_2Pb_8I_{21}$: C, 13.15; H, 0.89; N, 3.02 %; found: C, 13.41; H, 0.92; N, 3.13 %.

Crystallographic Studies. Single crystals of the title compounds were collected on a Bruker SMART

CCD-based diffractometer (Mo Kα radiation, λ = 0.71073 Å) at 293(2) K. The structures were solved by direct method and refined on F^2 by full-matrix least-squares method using the SHELXS-97 program.[1] All the non-hydrogen atoms were refined with anisotropic thermal parameters, and the hydrogen atoms of 2,2-bipy molecules were generated theoretically onto the specific carbon and nitrogen atoms and refined isotropically with fixed thermal factors. The crystallographic data for all the compounds are listed in Table S1-2 and important bond lengths are listed in Tables S3-S6.

Photocatalytic Activity Measurement. The photocatalytic activities of as-prepared samples were initially evaluated by the degradation of rhodamine B (RhB) a as model dye pollutants. In a typical process, 30 mg each sample of the compounds was added to a 30 mL of 1×10^{-5} mol·L^{-1} solution of organic pollutants. After being dispersed in an ultrasonic bath for 30 min, the mixture was then magnetically stirred in the dark for 10 hour before irradiation to ensure adsorption equilibrium between the catalyst and solution. The solution was then exposed to the visible light irradiation from a Xe lamp with distance 10 cm of between the Xe lamp and the reaction solution. The cut-off filter was used to remove all wavelengths less than 400 nm and more than 780 nm ensuring irradiation with visible-light only. Every 10 min, 4 mL of the mixture was continually taken from the reaction cell and the catalysts were separated from the suspensions by centrifugation. The degradation process was monitored through a wavelength scan on a GBC Cintra 2020 UV/Vis spectrophotometer. For collecting the adequate sample in recycling experiment, two or even more the photocatalytic processes were carried out under the same condition, and then the samples were separated through centrifugation. All the precipitates from the different processes were collected, combined and dried in an oven at 80 ºC for 12 h. After that, 30 mg of dried sample was performed for the second photocatalytic experiment according to the same method as that of first study. Other recycling experiment was also carried out with the same method. The light source in the above photoreactivity experiment was a 300 W Xe arc lamp (PLS-SXE300, Beijing Trusttech Co. Ltd).

Calculation Details. The density of state (DOS) of compound Fe@[Pb_8I_{21}] was calculated as represent by density functional theory (DFT) using the crystallographic data with the CASTEP code,

which uses a plane-wave basis set for the valence electrons and norm-conserving pseudopotential for the core electrons.[2] The number of plane waves included in the basis was determined by a cutoff energy of 320 eV, and the numerical integration of the Brillouin zone was performed using a 2 × 2 × 2 Monkhorst-Pack *k*-point. The other calculating parameters and convergence criteria were set by the default values of the CASTEP code, for example, an energy convergence tolerance of 1.0×10^{-5} eV.

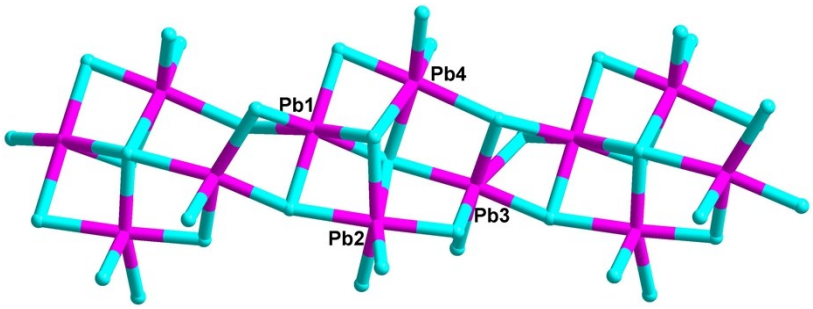

(a)

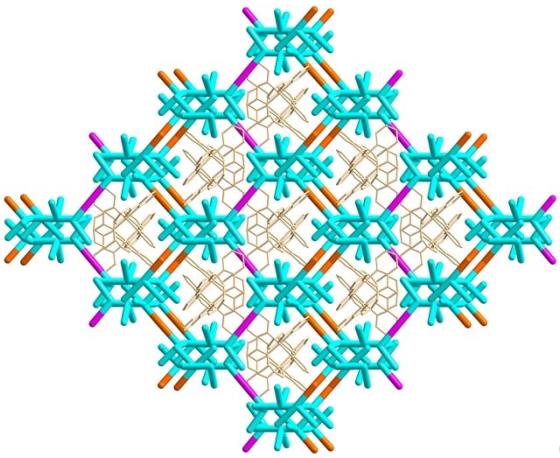

(b)

Fig. S1. Detailed view of the 1D $[Pb_4I_{12}]$ chain (a) and the 3D packing structure of compound $Fe@[Pb_8I_{21}]$.

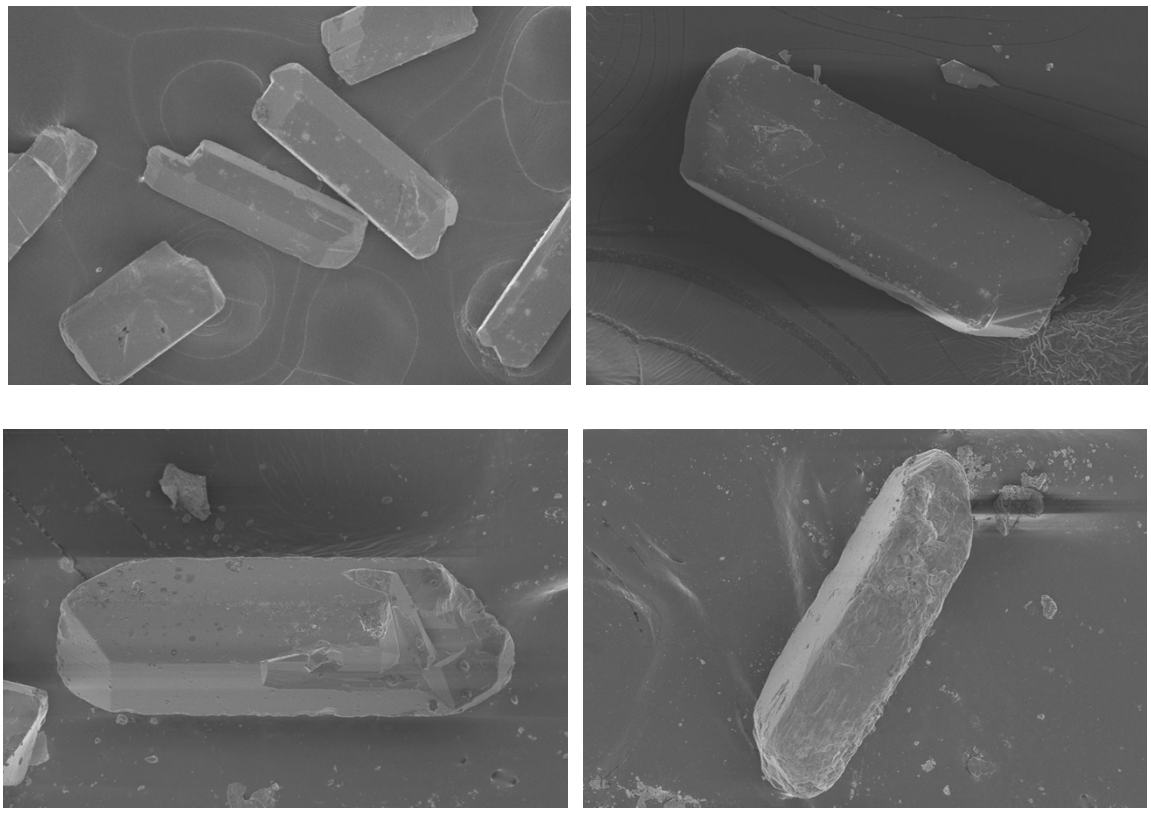

Fig. **S2**. The SEM images of prism-shaped single crystals of Co@[Pb_8I_{21}]. The images show the excellent prism-shaped single crystals of Co@[Pb_8I_{21}].

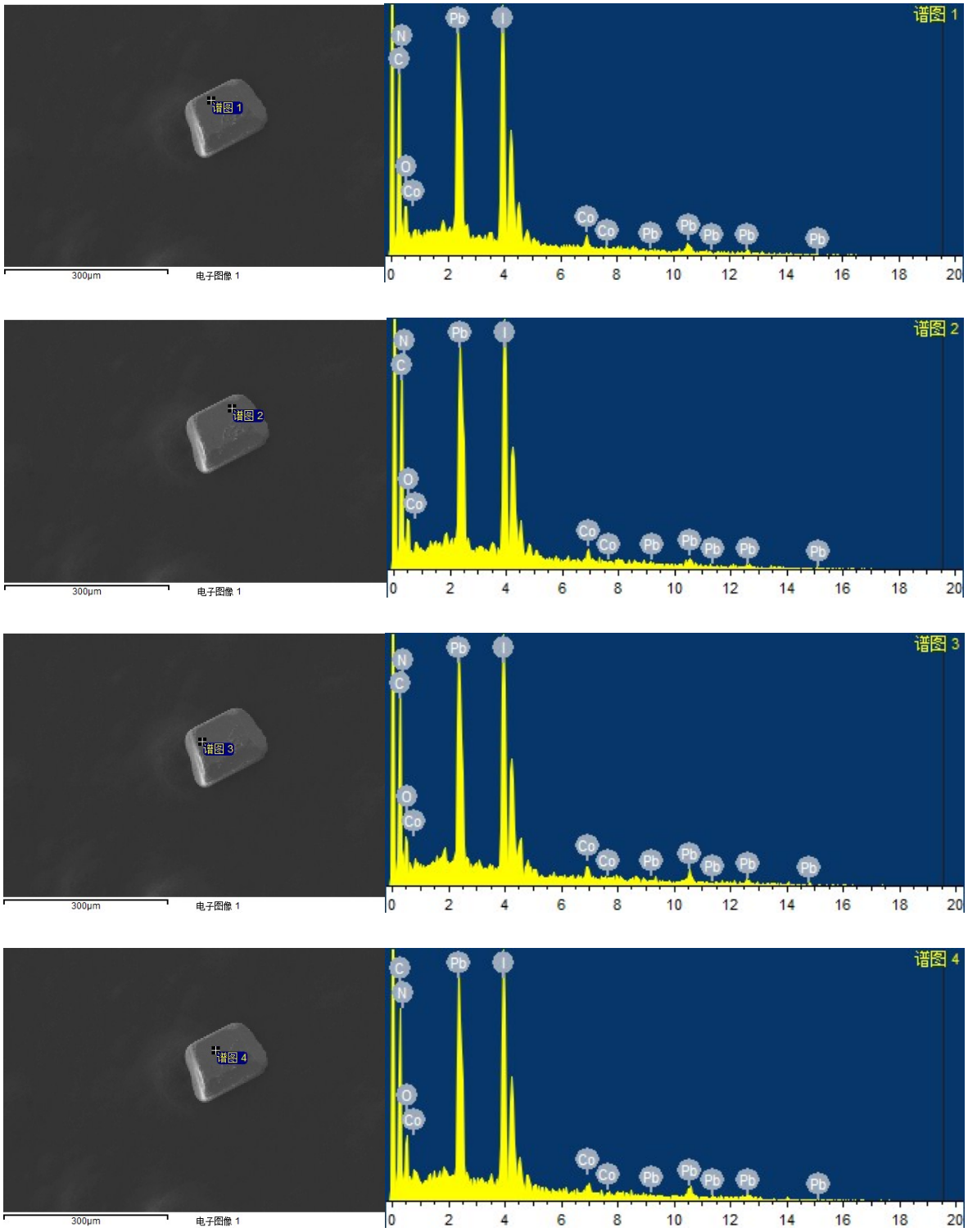

Fig. **S3**. The SEM images and Energy Dispersive Spectrometer (EDS) of crystal of Co@[Pb_8I_{21}]. The average Co/Pb/I molar ratios of 2.0 : 8.4 : 21.9 were in agreement with those determined by single crystal X-ray diffraction studies.

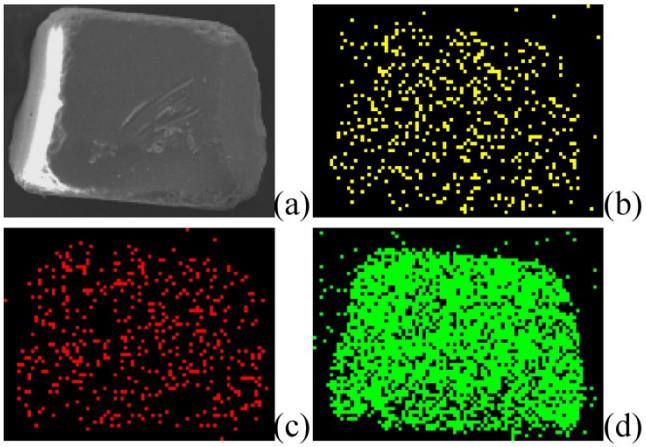

Fig. **S4**. Selected area and elemental mappings of Co (b), Pb (c) and I (d) for crystals of Co@[Pb_8I_{21}]. The elemental mapping shows that all elements are distributed uniformly on the surfaces of the crystals of Co@[Pb_8I_{21}].

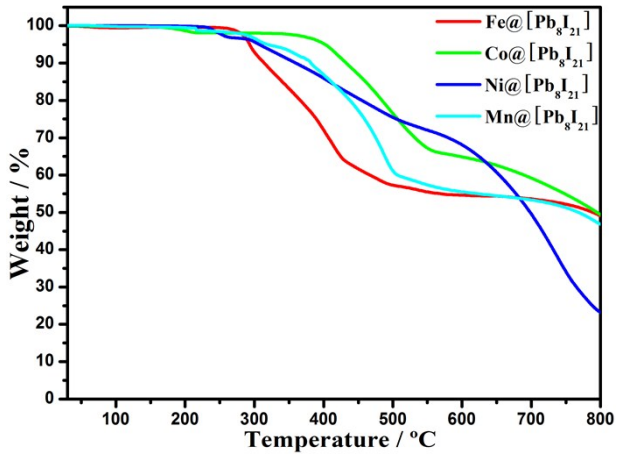

Fig. S5. Thermogravimetric analyses curves for compounds Fe@[Pb_8I_{21}], Co@[Pb_8I_{21}], Ni@[Pb_8I_{21}] and Mn@[Pb_8I_{21}]. The results show that TM@[Pb_8I_{21}] frameworks can be stable up to 240-270 °C for compounds Fe, Ni and Mn phases, while the compound Co@[Pb_8I_{21}] features higher stability and starts to decompose at about 370 °C. Such TM@[Pb_8I_{21}] framework is obviously more stable than those low-dimensional hybrid halides mainly originating from the 3D covalent network.[3-5]

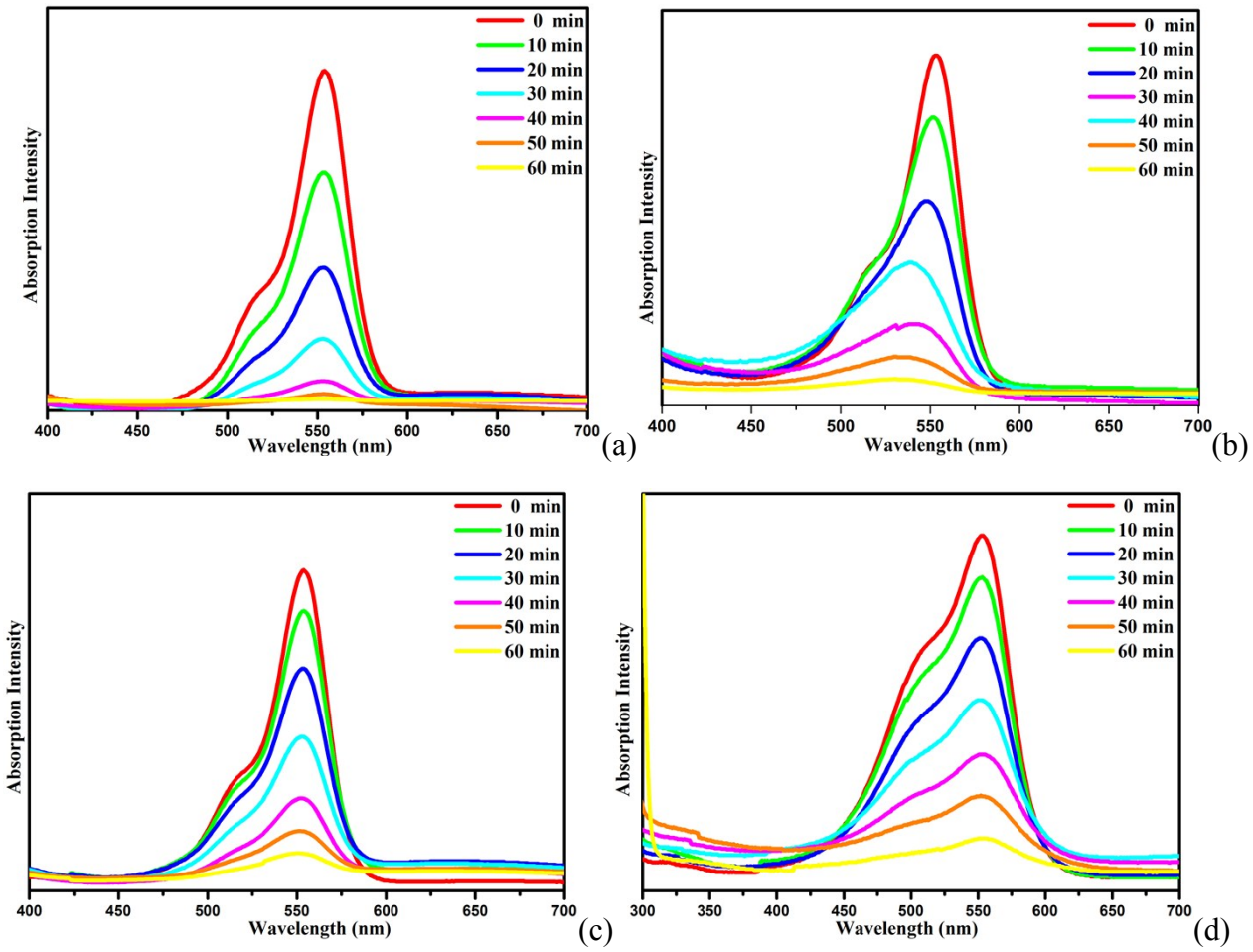

Fig. S6. The absorption spectra of the RhB solution in the photocatalytic effects of Fe@[Pb_8I_{21}] (a), Co@[Pb_8I_{21}] (b), Ni@[Pb_8I_{21}] (c) and Mn@[Pb_8I_{21}] (d) under the exposure to visible light.

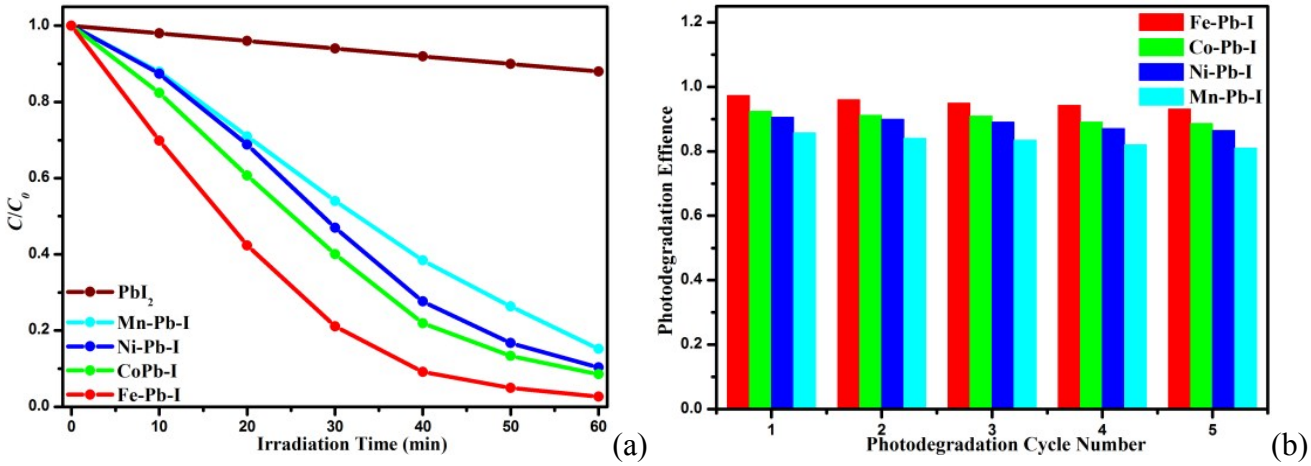

Fig. S7. The photodegradation ratios (C/C_0) of RhB under the irradiation of visible light (a) and the corresponding cycling degradation efficiencies of RhB by TM@[Pb_8I_{21}] (b).

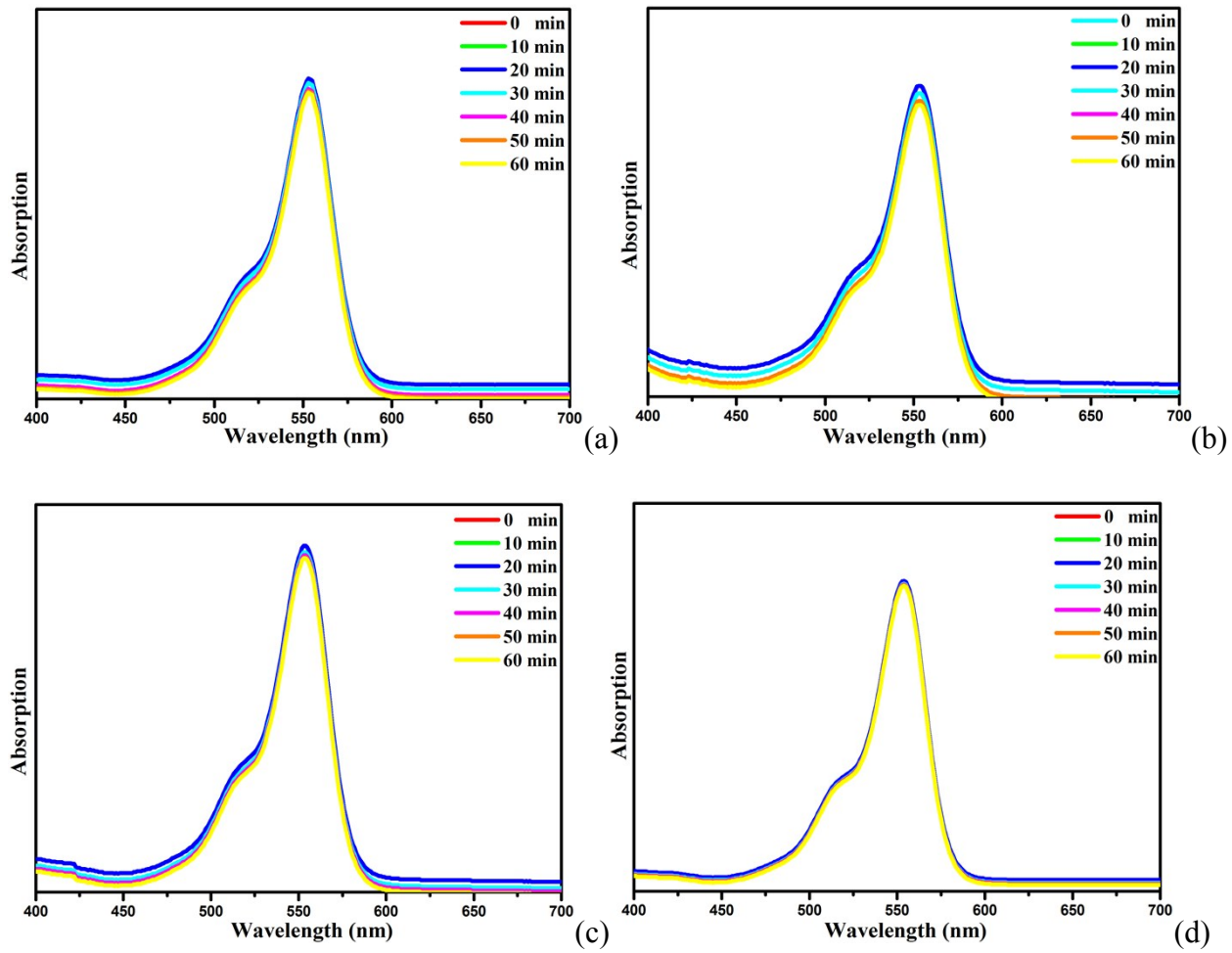

Fig. S8. The absorption spectra of the RhB solution in the photocatalytic effects of $[Fe(2.2\text{-bipy})_3]SO_4$ (a), $[Co(2.2\text{-bipy})_3](CH_3COO)_2$ (b), $[Ni(2.2\text{-bipy})_3](CH_3COO)_2$ (c) and $[Mn(2.2\text{-bipy})_3](CH_3COO)_2$ (d) under the exposure to visible light.

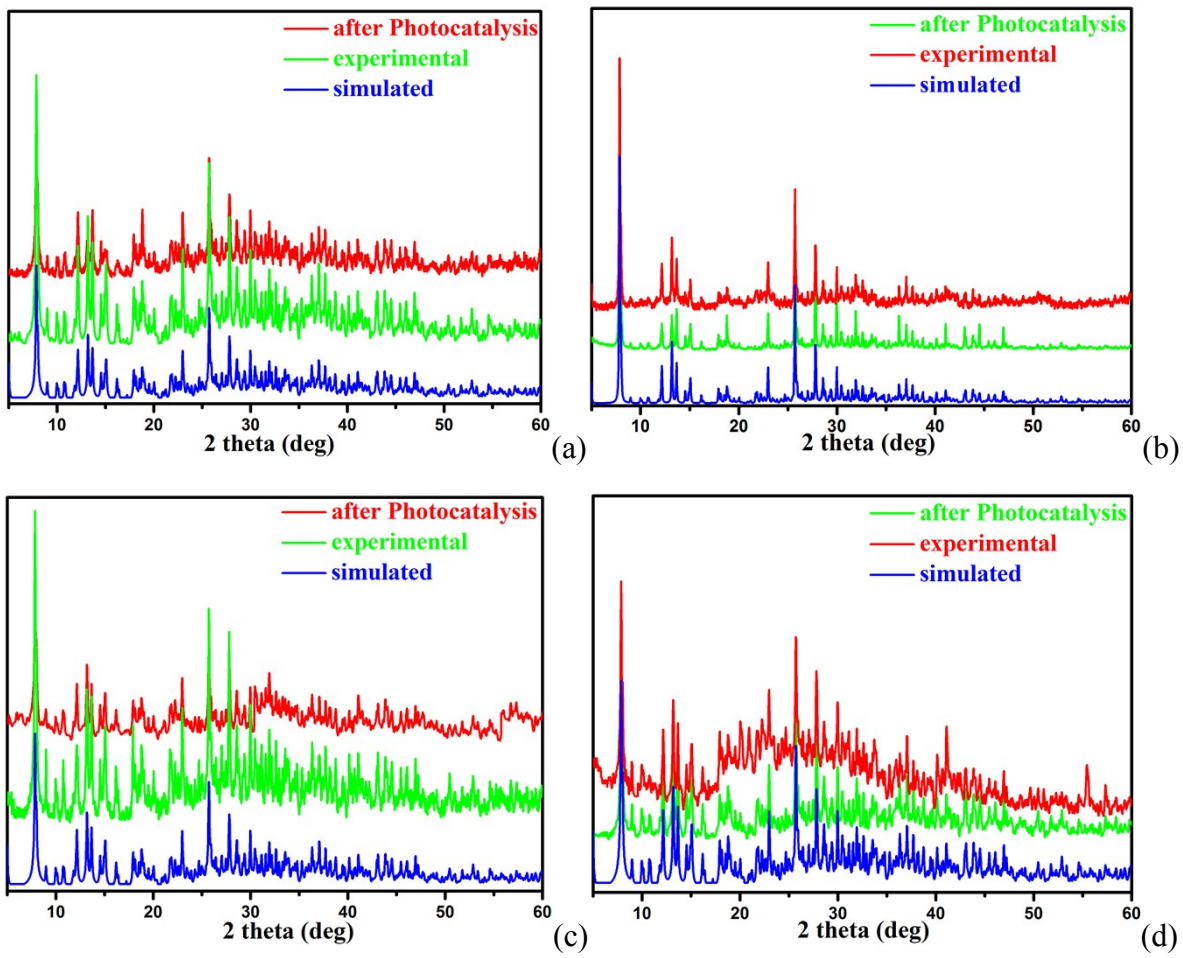

Fig. S9. The simulated, as-synthesized and powder X-ray diffraction patterns of Fe@[Pb_8I_{21}] (a), Co@[Pb_8I_{21}] (b), Ni@[Pb_8I_{21}] (c) and Mn@[Pb_8I_{21}] (d).

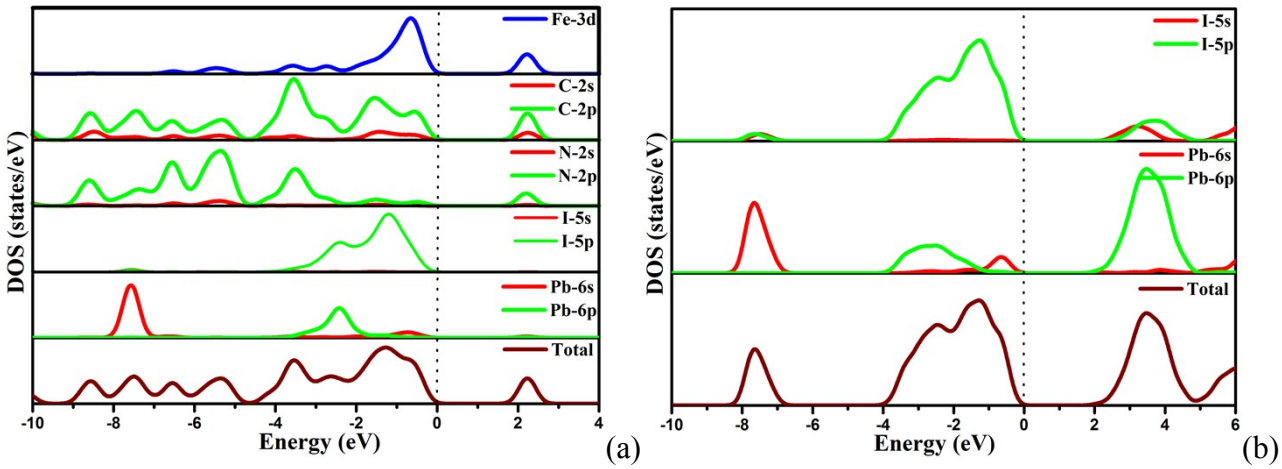

Fig. S10. Calculated total and partial DOS of compound Fe@[Pb_8I_{21}] (a) and PbI_2 (b).

Table S1. Crystal Data and Structure Refinements for compounds Fe@**[**Pb_8I_{21}**]** and Co@**[**Pb_8I_{21}**]**.

Compound	Fe@[Pb_8I_{21}]	Co@[Pb_8I_{21}]
chemical formula	$C_{60}N_{12}H_{49}Fe_2Pb_8I_{21}$	$C_{60}N_{12}H_{49}Co_2Pb_8I_{21}$
fw	5372.23	5377.38
Space group	$P2_1/c$	$P2_1/c$
a/Å	19.9674(10)	19.982(3)
b/Å	14.5362(7)	14.540(2)
c/Å	19.6748(10)	19.693(3)
β/°	117.5470(10)	117.564(2)
V(Å^3)	5063.2(4)	5071.9(13)
Z	2	2
D_{calcd} (g·cm^{-3})	3.524	3.521
Temp (K)	293(2)	293(2)
μ (mm^{-1})	19.966	19.973
F(000)	4628	4630
Reflections collected	58126	39406
Unique reflections	11509	11546
Reflections ($I>2\sigma(I)$)	7955	8778
GOF on F^2	1.038	1.052
R_1,wR_2	0.0647/0.1847	0.0656/0.1924
R_1,wR_2 (all data)	0.0972/0.2054	0.0789/0.2060

[a] $R_1 = \sum||F_o| - |F_c||/\sum|F_o|$, $wR_2 = \{\sum w[(F_o)^2 - (F_c)^2]^2/\sum w[(F_o)^2]^2\}^{1/2}$

Table S2. Crystal Data and Structure Refinements for compounds Ni@**[**Pb_8I_{21}**]** and Mn@**[**Pb_8I_{21}**]**.

Compound	Ni@[Pb_8I_{21}]	Mn@[Pb_8I_{21}]
chemical formula	$C_{60}N_{12}H_{49}Ni_2Pb_8I_{21}$	$C_{60}N_{12}H_{49}Mn_2Pb_8I_{21}$
fw	5377.95	5370.41
Space group	$P2_1/c$	$P2_1/c$
a/Å	19.9716(8)	19.9782(14)
b/Å	14.5395(6)	14.5401(10)
c/Å	19.6731(8)	19.6821(13)
β/°	117.54	117.5430(10)
V(Å^3)	5065.1(4)	5069.4(6)
Z	2	2
D_{calcd} (g·cm^{-3})	3.526	3.518
Temp (K)	293(2)	293(2)
μ (mm^{-1})	20.044	19.905
F(000)	4636	4624
Reflections collected	57862	58296
Unique reflections	11459	11591
Reflections ($I>2\sigma(I)$)	7479	7611
GOF on F^2	1.021	1.028
R_1,wR_2	0.0622/0.1629	0.0633/0.1822
R_1,wR_2 (all data)	0.1027/0.1878	0.1028/0.2088

[a] $R_1 = \sum||F_o| - |F_c||/\sum|F_o|$, $wR_2 = \{\sum w[(F_o)^2 - (F_c)^2]^2/\sum w[(F_o)^2]^2\}^{1/2}$

Table S3. Selected bond lengths (Å) for compound Fe@[Pb_8I_{21}].

Pb(1)-I(6)	3.0746(12)	Pb(3)-I(5)#1	3.0973(13)

Pb(1)-I(3)	3.1182(12)	Pb(3)-I(2)	3.1806(12)
Pb(1)-I(1)	3.1797(11)	Pb(3)-I(8)#2	3.2280(13)
Pb(1)-I(2)	3.2046(12)	Pb(3)-I(4)	3.2719(12)
Pb(1)-I(4)	3.505	Pb(3)-I(6)	3.534
Pb(1)-I(10)	3.647	Pb(3)-I(10)	3.472
Pb(2)-I(7)	3.0006(13)	Pb(4)-I(9)	3.0085(18)
Pb(2)-I(5)	3.1061(12)	Pb(4)-I(1)	3.1074(12)
Pb(2)-I(8)	3.2040(14)	Pb(4)-I(3)	3.591
Pb(2)-I(2)	3.3686(12)	Pb(4)-I(10)	3.602
Pb(2)-I(3)	3.586	Pb(4)-I(4)	3.549
Pb(2)-I(10)	3.483	Pb(4)-I(11)	3.474

Symmetry transformations used to generate equivalent atoms: #1 *x*, -*y*+3/2, *z*+1/2, #2 -*x*+1, -*y*+1, -*z*+1.

Table S4. Hydrogen bonds data for compound Fe@**[**Pb_8I_{21}**]**.

D-H···A	d(D-H)	d(H···A)	d(D···A)	<(DHA)
C(1)-H(1)···N(6)	0.93	2.49	2.9855	114
C(4)-H(4)···I(7)	0.93	2.95	3.7151	141
C(10)-H(10)···N(5)	0.93	2.50	3.0304	116
C(11)-H(11)···N(1)	0.93	2.45	2.9596	115
C(12)-H(12)···I(7)	0.93	2.88	3.7392	155
C(20)-H(20)···N(4)	0.93	2.54	3.0473	115
C(21)-H(21)···N(2)	0.93	2.50	3.0117	115
C(22)-H(22)···I(1)	0.93	2.98	3.8148	150
C(30)-H(30)···N(3)	0.93	2.48	2.9654	113

Table S5. Selected bond lengths (Å) for compound Co@**[**Pb_8I_{21}**]**.

Pb(1)-I(6)	3.0720(14)	Pb(3)-I(5)#1	3.0976(15)

Pb(1)-I(3)	3.1171(13)	Pb(3)-I(2)	3.1792(14)
Pb(1)-I(1)	3.1807(13)	Pb(3)-I(8)#2	3.2253(15)
Pb(1)-I(2)	3.2043(14)	Pb(3)-I(4)	3.2733(14)
Pb(1)-I(4)	3.505	Pb(3)-I(6)	3.534
Pb(1)-I(10)	3.647	Pb(3)-I(10)	3.472
Pb(2)-I(7)	2.9997(15)	Pb(4)-I(9)	3.007(2)
Pb(2)-I(5)	3.1041(14)	Pb(4)-I(1)	3.1043(14)
Pb(2)-I(8)	3.2052(16)	Pb(4)-I(3)	3.591
Pb(2)-I(2)	3.3652(13)	Pb(4)-I(4)	3.549
Pb(2)-I(3)	3.586	Pb(4)-I(1)	3.474
Pb(2)-I(10)	3.483	Pb(4)-I(10)	3.602

Symmetry transformations used to generate equivalent atoms: #1 *x*, -*y*+1/2, *z*-1/2, #2 -*x*, -*y*+1, -*z*.

Table S6. Hydrogen bonds data for compound Co@**[**Pb_8I_{21}**]**.

D-H···A	d(D-H)	d(H···A)	d(D···A)	<(DHA)
C(1)-H(1)···N(6)	0.93	2.46	2.9570	113
C(4)-H(4)···I(7)	0.93	2.95	3.7065	139
C(10)-H(10)···N(3)	0.93	2.53	3.0456	116
C(11)-H(11)···N(1)	0.93	2.42	2.9457	116
C(12)-H(12)···I(7)	0.93	2.87	3.7194	153
C(20)-H(20)···N(5)	0.93	2.55	3.0547	115
C(21)-H(21)···N(2)	0.93	2.50	3.0106	115
C(22)-H(22)···I(1)	0.93	2.97	3.7929	148
C(30)-H(30)···N(4)	0.93	2.48	2.9787	114

Table S7. Selected bond lengths (Å) for compound Ni@**[**Pb_8I_{21}**]**.

Pb(1)-I(6)	3.0741(14)	Pb(3)-I(7)#1	3.0975(14)

Pb(1)-I(8)	3.1160(13)	Pb(3)-I(10)	3.1796(13)
Pb(1)-I(11)	3.1800(12)	Pb(3)-I(4)#2	3.2254(15)
Pb(1)-I(10)	3.2085(13)	Pb(3)-I(9)	3.2719(14)
Pb(1)-I(2)	3.643	Pb(3)-I(2)	3.475
Pb(1)-I(9)	3.505	Pb(3)-I(6)	3.535
Pb(2)-I(5)	3.0005(14)	Pb(4)-I(3)	3.0053(19)
Pb(2)-I(7)	3.1029(14)	Pb(4)-I(1)	3.092(3)
Pb(2)-I(4)	3.2073(15)	Pb(4)-I(11)	3.1042(14)
Pb(2)-I(10)	3.3658(13)	Pb(4)-I(9)	3.550
Pb(2)-I(2)	3.479	Pb(4)-I(2)	3.608
Pb(2)-I(8)	3.585	Pb(4)-I(8)	3.594

Symmetry transformations used to generate equivalent atoms: #1 *x*, -*y*+1/2, *z*-1/2, #2 -*x*, -*y*, -*z*.

Table S8. Hydrogen bonds data for compound Ni@**[**Pb_8I_{21}**]**.

D-H···A	d(D-H)	d(H···A)	d(D···A)	<(DHA)
C(1)-H(1)···N(3)	0.93	2.51	3.0287	116
C(3)-H(3)···N(2)	0.93	2.52	3.0316	115
C(4)-H(4)···N(5)	0.93	2.56	3.0527	114
C(7)-H(7)···N(4)	0.93	2.47	2.9715	114
C(12)-H(12)···N(1)	0.93	2.50	3.0137	115
C(16)-H(16)···I(11)	0.93	2.99	3.8206	150
C(26)-H(26)···I(5)	0.93	2.93	3.6884	140
C(27)-H(27)···I(5)	0.93	2.91	3.7613	153
C(31)-H(31)···N(6)	0.93	2.47	2.9661	113

Table S9. Selected bond lengths (Å) for compound Mn@**[**Pb_8I_{21}**]**.

Pb(1)-I(5)	3.0747(15)	Pb(3)-I(2)#1	3.1000(15)

Pb(1)-I(4)	3.1182(14)	Pb(3)-I(1)	3.1809(14)
Pb(1)-I(11)	3.1806(13)	Pb(3)-I(7)#2	3.2279(16)
Pb(1)-I(1)	3.2080(14)	Pb(3)-I(3)	3.2731(15)
Pb(1)-I(3)	3.507	Pb(3)-I(9)	3.474
Pb(1)-I(9)	3.648	Pb(3)-I(5)	3.535
Pb(2)-I(6)	3.0000(15)	Pb(4)-I(8)	3.005(2)
Pb(2)-I(2)	3.1051(14)	Pb(4)-I(11)	3.1071(14)
Pb(2)-I(7)	3.2070(16)	Pb(4)-I(10)	3.477
Pb(2)-I(1)	3.3651(14)	Pb(4)-I(4)	3.595
Pb(2)-I(4)	3.587	Pb(4)-I(3)	3.547
Pb(2)-I(9)	3.481	Pb(4)-I(9)	3.609

Symmetry transformations used to generate equivalent atoms: #1 *x*, -*y*+1/2, *z*-1/2, #2 -*x*, -*y*+1, -*z*.

Table S10. Hydrogen bonds data for compound Mn@**[**Pb_8I_{21}**]**.

D-H···A	d(D-H)	d(H···A)	d(D···A)	<(DHA)
C(1)-H(1)···N(3)	0.93	2.45	2.9629	115
C(2)-H(2)···I(6)	0.93	2.89	3.7466	153
C(10)-H(10)···N(5)	0.93	2.53	3.0348	115
C(11)-H(11)···N(4)	0.93	2.52	3.0442	116
C(17)-H(17)···I(6)	0.93	2.93	3.6956	141
C(20)-H(20)···N(6)	0.93	2.50	2.9835	112
C(21)-H(21)···N(3)	0.93	2.51	2.9926	113
C(29)-H(29)···I(11)	0.93	2.97	3.8074	151
C(30)-H(30)···N(2)	0.93	2.53	3.0253	114

Table S11. Comparison of the distortion degree of [PbX_6] octahedral units in 3D Pb-X frameworks.

Framework	atom	Pb-X lengths (Å)			Average Pb-X lengths (Å)	distortion degree	Ref
$[PbI_3]^-$	Pb(1)	3.153	3.153	3.153	3.153	0	6
		3.153	3.153	3.153			
$[Pb_2Cl_6]^{2-}$	Pb(1)	2.850	2.836	2.808	2.884	3.8022E-4	7
		2.961	2.940	2.910			
$[Pb_7Br_{18}]^{4-}$	Pb(1)	3.006	3.011	3.052	3.023	4.6470E-5	8
		3.006	3.011	3.052			
	Pb(2)	3.079	2.959	2.918	3.006	5.4921E-4	
		2.936	3.093	3.051			
	Pb(3)	2.957	2.911	3.054	3.103	0.0026	
		3.39	3.198	3.107			
	Pb(4)	2.978	2.936	3.180	3.083	9.2584E-4	
		3.099	3.173	3.132			
$[Pb_7I_{18}]^{4-}$	Pb(1)	3.190	3.310	3.527	3.247	0.0024	9
		3.283	3.171	3.004			
	Pb(2)	3.276	3.163	3.161	3.225	2.6231E-4	
		3.204	3.292	3.255			
	Pb(3)	3.191	3.20	3.143	3.224	3.2337E-4	
		3.291	3.209	3.309			
	Pb(4)	3.130	3.209	3.348	3.229	7.7885E-4	
		3.130	3.209	3.348			
$[Pb_9Br_{20}]^{2-}$	Pb(1)	2.857	2.953	3.065	3.006	9.9766E-4	10
		2.953	3.065	3.145			
	Pb(2)	3.423	3.063	3.063	3.068	0.00304	
		2.890	2.985	2.985			
	Pb(3)	3.078	2.972	2.933	3.023	4.6689E-4	
		3.102	3.078	2.972			
	Pb(4)	3.007	3.007	2.993	3.002	4.8320E-6	
		3.007	3.007	2.993			
$[Pb_8I_{21}]$	Pb(1)	3.075	3.118	3.180	3.288	0.0042	This work
		3.205	3.505	3.647			
	Pb(2)	3.001	3.106	3.204	3.291	0.0039	
		3.369	3.586	3.483			
	Pb(3)	3.097	3.181	3.228	3.297	0.0022	
		3.272	3.534	3.472			
	Pb(4)	3.008	3.107	3.591	3.389	0.0050	
		3.602	3.549	3.474			

Reference.

1. G. M. Sheldrick, SHELXTL, University of Göttingen, Göttingen, 2001.

2. M. D. Segall, P. J. D. Lindan, M. J. Probert, C. J. Pickard, P. J. Hasnip, S. J. Clark, M. C. Payne, *J. Phys.: Condens. Matter*, 2002, **14**, 2717–2744.

3. S. L. Li, F. Q. Zhang and X. M. Zhang, *Chem. Commun*., 2015, **51**, 8062-8065.

4. Y. R. Qiao, P. F. Hao and Y. L. Fu, *Inorg. Chem*. 2015, **54**, 8705-8710.

5. S. L. Li and X. M. Zhang, *Inorg. Chem*. 2014, **53**, 8376-8383.

6. *J. Phys. Chem. Lett.*, 2016, **7**, 2412–2419.

7. G. E Wang, G. Xu, M. S. Wang, L. Z. Cai, W. H. Li, G. C. Guo, *Chem. Sci*., 2015, **6**, 7222–7226.

8. X. X. Li, T. T. H. Do, A. G. del Águila, Y. J. Huang, W. Q. Chen, Q. H. Xiong, Q. C. Zhang, *Chem. Asian J*., 2018, **13**, 3185-3189.

9. Z. J. Zhang, S. C. Xiang, G. C. Guo, G. Xu, M. S. Wang, J. P. Zou, S. P. Guo, J. S. Huang, *Angew. Chem. Int. Ed*. 2008, **47**, 4149-4152.

10. G. F. Liu, P. Y. Gu, L. N. Nie, Q. C. Zhang, *Chem. Commun*., 2017, 53, 12365-12368.